

On the Nature of the CP Bond in Phosphaalkynes

Maria F. Lucas, Maria C. Michelini, Nino Russo,* and Emilia Sicilia

Dipartimento di Chimica and Centro di Calcolo ad Alte Prestazioni per Elaborazioni Parallele e, Distribuite-Centro d'Eccellenza MURST, Università della Calabria, I-87030 Arcavacata di Rende, Italy

Received October 19, 2007

Abstract: In this work, we report results of calculations based on the density functional theory (B3LYP/6-311+G(2d,2p)) of different species containing a terminal cyaphide bond. The chosen species range from small molecules and anions ($\text{C}\equiv\text{P}^-$, $\text{HC}\equiv\text{P}$, $t\text{BuC}\equiv\text{P}$, $[(\text{CF}_3)_3\text{BC}\equiv\text{P}]^-$) to large transition-metal containing complexes ($[(\text{dppe})_2\text{Ru}(\text{H})(\text{C}\equiv\text{P})]$, *trans*- $[\text{Pt}(\text{PMe}_3)_2(\text{Cl})(\text{C}\equiv\text{P})]$, *trans*- $[\text{Pt}(\text{PMe}_3)_2(\text{Cl})(\text{CP})\text{Pt}(\text{PMe}_3)_2]$). A comparative analysis of the description of the $\text{C}\equiv\text{P}$ bond obtained by different methodologies is presented. Topological analyses of the electron density in the framework of the theory of atoms in molecules (AIM) and of the electron localization function (ELF) are complemented with the results obtained by natural bond orbital analysis (NBO).

1. Introduction

For many years it was accepted that thermally stable compounds containing multiple bonds would occur only for elements of the second period. The so-called “double-bond rule” stated that compounds with multiple bonds involving heavy main-group elements were unstable. This rule was based on the fact that the σ bonds for heavy elements are relatively long and the increasingly diffuse nature of p orbitals makes for poor overlap to form π bonds. However, early experimental studies clearly established that new compounds having (p–p) π bonds could be synthesized provided some criteria were taken into account. In particular, it was shown that this type of π systems could be stabilized by resonance, by reduction of the polarity in the π systems and avoiding the oligomerization reactions.¹ In the last years, the refinement of experimental techniques has permitted the synthesis and characterization of compounds with multiple phosphorus-element bonds and the detailed study, both from experimental and theoretical viewpoints, of their molecular and electronic structure became a very exciting area in organophosphorus chemistry.

In spite of the discovery, which was considered mostly a curiosity, of the phosphaalkyne HCP by Gier in 1961² only 20 years later³ with the synthesis of *t*BuCP, a surprisingly thermally stable compound, the chemistry of phosphaalkynes was firmly established. The synthesis of this compound

proved to be the starting point for the rapid development of the chemistry of the $\text{C}\equiv\text{P}$ bond. Soon it became clear that phosphaalkynes can be stabilized in several ways, and today a whole range of species containing $\text{C}\equiv\text{P}$ triple bonds is known.

Stabilization of the phosphaalkyne group for the synthesis of isolable $\text{R}-\text{C}\equiv\text{P}$ species is achieved in most cases by steric shielding using large substituents, as the *tert*-butyl one, otherwise the triple $\text{C}\equiv\text{P}$ bond polymerizes.⁴ As a result, many phosphaalkynes have been synthesized and subsequently incorporated as ligands into transition-metal complexes.^{5–8} The ligand was stabilized as a μ_2 -bridging ligand in dinuclear complexes in which the carbon atom is coordinated to two platinum or two iron atoms.^{6,7} Only recently, the synthesis and characterization of a transition-metal complex⁸ with a terminal cyaphide has raised again the challenging problem of the stabilization and, therefore, isolation of transition-metal complexes containing a terminal $\text{C}\equiv\text{P}^-$ ligand.

In addition to some early works on the subject,⁹ several theoretical studies have been performed in the last years on species containing the triple $\text{C}\equiv\text{P}$ bond.¹⁰ Hübler and Schwerdtfeger have performed a theoretical analysis of the vibrational frequencies and the NMR chemical shifts (³¹P and ¹³C), of a range of λ^3 -phosphaalkynes.^{10a} Kurita and co-workers presented MP2 and B3LYP calculations on several compounds containing single and multiple CP bonds, among which are HCP, CH_3CP , and *t*BuCP.^{10b} Pascoli and Lavendy

* Corresponding author e-mail: nrusso@unical.it.

reported a DFT study of C_nP , C_nP^+ , and C_nP^- ($n = 1-7$) clusters.^{10c} More recently, M6 and collaborators have performed a combined theoretical and experimental work concerning the gas-phase acidity of HCP, CH_3CP , HCAs, and CH_3CAs .^{10d}

In the present work, the chemical nature of the $C\equiv P$ bond in a series of phosphalkynes was investigated using different bonding analysis methodologies. A comparison of the different bonding descriptions is provided. The molecular structures and vibrational frequencies obtained using density functional theory were compared to the experimental available data.

2. Computational Details

Geometry optimizations as well as frequency calculations for all the examined phosphalkynes were performed at the Density Functional level of theory as implemented by GAUSSIAN03 code.¹¹ The Becke's three-parameter hybrid functional¹² combined with the Lee, Yang, and Parr (LYP) correlation functional,¹³ denoted as B3LYP, was used. For Pt and Ru LanL2DZ effective core potentials¹⁴ were adopted in conjunction with their split valence basis sets. The standard 6-311+G(2d,2p) basis sets of Pople and co-workers were employed for the rest of the atoms.¹⁵ The same level of theory was also used to obtain the wavefunctions of all the structures.

The bonding features of all the studied species were analyzed by means of Natural Bond Orbital (NBO) and Natural Population Analysis (NPA).¹⁶ We have also analyzed the nature of the bonding by using two different topological methodologies, namely, the topological analysis of the electron localization function (ELF) and the Atoms in Molecules (AIM) approach. ELF analysis is based on the topology of the gradient vector field of the Becke and Edgecombe¹⁷ electron localization function, as implemented by Silvi and Savin.¹⁸ The ELF, $\eta(\mathbf{r})$, can be interpreted as a measure of the electron localization in atomic and molecular systems, namely, as the conditional probability of finding two electrons with the same spin around a reference point. The analysis of the ELF gradient field provides a mathematical model enabling the partition of the molecular position space in basins of attractors (Ω_A), which present in principle a one-to-one correspondence with chemical local objects such as bonds and lone pairs. These basins are either core basins, usually labeled C(A), or valence basins, V(A,...), belonging to the outermost shell and characterized by the number of core basins with which it shares a common boundary, which is called the synaptic order. In this representation the monosynaptic basins correspond to nonbonded pairs of the usual Lewis representation, whereas the di- and polysynaptic basins are related to bonds. The presence of di- or polysynaptic basins is indicative of shared interactions (covalent, dative, metallic bonds), whereas the absence of these basins is indicative of closed-shell interactions (ionic, hydrogen, van der Waals bonds). The electronic population of a synaptic basin, $\bar{N}(\Omega_A)$, is obtained as the integral of the one-electron density over the basin. The variance of the basin population, $\sigma^2[\bar{N}(\Omega_A)]$, that is the square of the standard deviation of the population, represents the quantum-mechanical uncer-

tainty of the basin population and is a result of the delocalization of electrons. It has the meaning of an excess in the number of pairs due to the interaction of Ω_A with the other basins and is usually written as the sum of contributions of all other basins.

Within ELF analysis a multiple bond is characterized by a basin population $\bar{N}(\Omega_A)$ higher than 2.0 electrons and a variance $\sigma^2[\bar{N}(\Omega_A)]$ less than the corresponding basin population.

The TopMod package was used to analyze the topology of the ELF function.¹⁹

AIM analysis²⁰ explores the topology of the electron density, $\rho(\mathbf{r})$, of the molecules revealing insightful information on the nature of the bonds. A (3, -1) critical point of the electron density, $\rho(\mathbf{r})$, located between two atomic centers denotes the presence of a bond. Topologically, this corresponds to a point in the real space where the gradient of $\rho(\mathbf{r})$, $\nabla\rho(\mathbf{r})$, is zero and where the curvature of $\rho(\mathbf{r})$, expressed through three eigenvalues of the diagonalized Hessian of $\rho(\mathbf{r})$, is positive for an eigenvector linking two atomic centers (λ_3) and negative for the two others (λ_1, λ_2) perpendicular to it. Unequal values of λ_1 and λ_2 at the (3, -1) bond critical points (BCPs) denote an anisotropic spread of electrons quantified through the concept of ellipticity, which is defined as

$$\epsilon = (\lambda_1/\lambda_2) - 1$$

(with $\lambda_1 > \lambda_2$). According to the mathematical definition, values of ϵ greater than zero indicate partial π -character in a bond or electronic distortion away from σ -symmetry along the path.²¹ Double bonds are usually characterized by significant ellipticity values, as it is found for C,C double bonds,^{21b} whereas in the case of triple bonds, and due to the cylindrical symmetry resulting from the presence of two π -bonds, that values are expected to be very close to zero.

The most used property to evaluate the characteristics of the bond is the Laplacian of the charge density, $\nabla^2\rho(\text{bcp})$. When $\nabla^2\rho(\text{bcp}) < 0$, charge is concentrated at the critical point, while when $\nabla^2\rho(\text{bcp}) > 0$, charge is locally depleted.

Within the framework of AIM analysis the variance, $\sigma^2(\Omega_A)$, can also be spread in terms of the contribution from other basins, the covariance, $\text{cov}(\Omega_A, \Omega_B)$, which has a clear relationship with the so-called delocalization index, $\delta(\Omega_A, \Omega_B)$ ²²

$$\text{cov}(\Omega_A, \Omega_B) = -\delta(\Omega_A, \Omega_B)/2$$

The delocalization index accounts for the electrons delocalized or shared between the basins Ω_A and Ω_B . This index, in the single determinant approach, is exactly the topological bond order defined by Ángayán and co-workers.²³ We must mention, however, that even when for molecular bonds with equally shared pairs a simple relationship between the delocalization index and the formal bond order (number of Lewis bonded pairs) has been generally found,^{22a} for polar bonds there is no longer such a simple relationship. It has been shown that the delocalization index tends to decrease with the increased electronegativity difference of the atoms involved in the bond. There has been some discussion in the past regarding the use of this index as a covalent bond order.²⁴

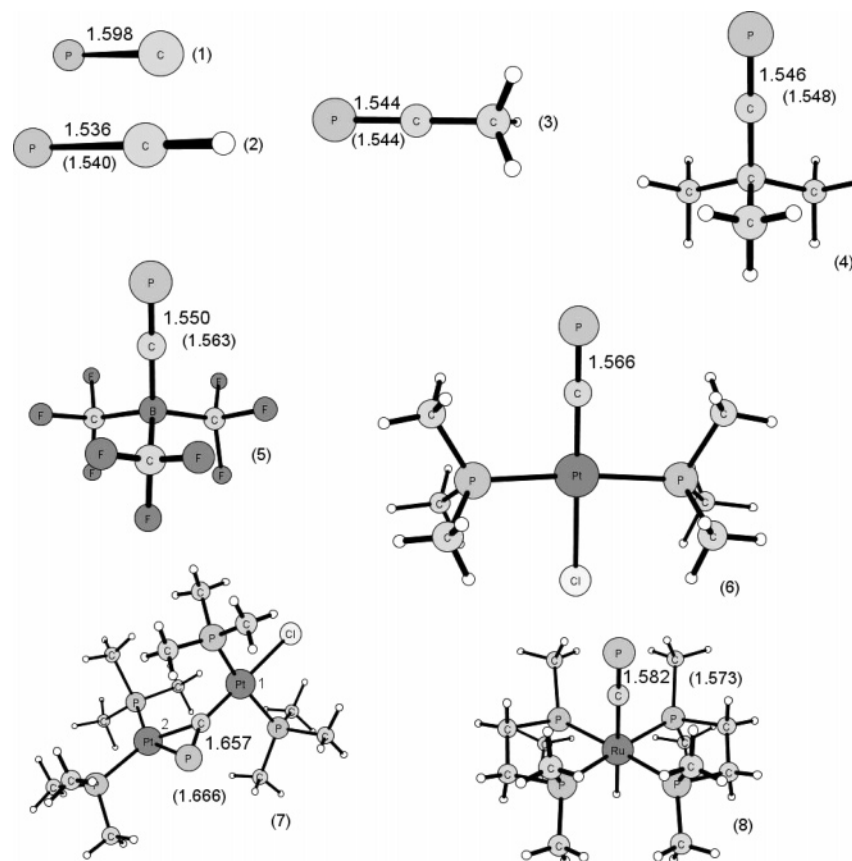


Figure 1. Optimized CP bond length of (1) CP^- ; (2) HCP; (3) CH_3CP ; (4) $t\text{BuCP}$; (5) $[(\text{CF}_3)_3\text{BPC}]^-$; (6) $\text{trans}[\text{Pt}(\text{PMe}_3)_2(\text{Cl})(\text{CP})]$; (7) $\text{trans}[\text{Pt}(\text{PMe}_3)_2(\text{Cl})(\text{CP})\text{Pt}(\text{PMe}_3)_2]$; and (8) $[(\text{dppe})_2\text{Ru}(\text{H})(\text{CP})]$. For the sake of comparison, available experimental values are also reported in parentheses.

The BCPs were primarily localized with the EXTREME program (part of the AIMPAC package)²⁰ and verified with the TopMod program.¹⁹

3. Results and Discussion

We have initiated the study of the $\text{C}\equiv\text{P}$ bond with CP^- (1), HCP (2), and CH_3CP (3). The optimized structures of these compounds are shown in Figure 1, and their Cartesian coordinates are included as Supporting Information.

Previous calculations on (1) show a $\text{C}\equiv\text{P}$ bond of 1.609 Å for an optimization at the B3LYP/6-311G(d) level^{10c} and 1.604 Å at QCISD/6-311G+(df,p),^{10d} while we have a calculated value of 1.598 Å which is in good agreement with previous results. For HCP, at the QCISD/6-311G(d) level, the $\text{C}\equiv\text{P}$ bond was previously found to be 1.544 Å,^{10d} our calculations indicate 1.536 Å, and for CH_3CP the value is 1.549 Å^{10d} in comparison with a value of 1.544 Å calculated by us. Our computations are then consistent with previous calculations as well as with experimental microwave data for HCP (1.5404 Å)^{25a} and CH_3CP (1.544(4) Å).^{25b}

The frequency analysis also retrieved vibrational frequencies for the $\text{C}\equiv\text{P}$ bond stretching consistent with experimental data and with previous calculations. For CP^- the calculated value of 1197 cm^{-1} is similar to the previously calculated^{10d} one of 1198 cm^{-1} , and the same takes place for (2) and (3) with values calculated by us of 1335 cm^{-1} and 1591 cm^{-1} in good agreement with previously calculated 1327 cm^{-1} and 1616 cm^{-1} values, respectively.^{10d} The

lengthening of the $\text{C}\equiv\text{P}$ bond as a consequence of deprotonation is expected for CP^- ; however, the calculated vibrational frequency (1335 cm^{-1}) is overestimated with respect to the 1265 cm^{-1} assigned experimental value.²

For $t\text{BuCP}$ (4) experimental data are available as well as some theoretical calculations at the RHF/6-31G(d) level.²⁶ That calculations established a bond distance of 1.519 Å for the CP bond which is close to the experimental diffraction data of 1.548(1) Å.²⁶ Our calculations assign a $\text{C}\equiv\text{P}$ bond distance of 1.546 Å which is very close to the expected experimental value. The vibrational frequency value of 1573 cm^{-1} is consistent with the experimental value (1533 cm^{-1}).²⁷

We have also optimized $[(\text{CF}_3)_3\text{BC}\equiv\text{P}]^-$, structure 5 in Figure 1, which is structurally similar to $t\text{BuCP}$. The $\text{C}\equiv\text{P}$ bond was calculated to be 1.550 Å, and the frequency analysis estimated a stretching mode at 1500 cm^{-1} that is in good agreement with a bond distance of 1.563(10) Å and a vibrational mode at 1468 cm^{-1} from experimental data.²⁷

In the present work, we have also investigated the characteristics of the $\text{C}\equiv\text{P}$ bond in some metal complexes of platinum and ruthenium. The compound $\text{trans}[\text{Pt}(\text{PET}_3)_2(\text{Cl})(\text{C}\equiv\text{P})]$ (6) was the first transition-metal complex containing a terminal $\text{C}\equiv\text{P}$ ligand to be synthesized.⁷ However, no structural data are available for this compound, since it is too unstable to be isolated, and for this reason theoretical investigations can be very helpful. To save computer time the ethyl (Et) groups were substituted with methyl (Me) ones. We have established that the $\text{C}\equiv\text{P}$ bond

Table 1. C≡P Stretching Harmonic Calculated and Experimental Vibrational Frequencies (cm⁻¹) and Natural Atomic and AIM (in Parentheses) Charges on Carbon and Phosphorus Atoms

	calcd freq	exptl freq	C atom charge	P atom charge
CP ⁻	1197	—	-0.83 (-1.29)	-0.17 (0.40)
HCP	1335	1265 ^a	-0.73 (-1.17)	0.52 (1.05)
CH ₃ CP	1591	1559 ^b	-0.51 (-1.06)	0.49 (0.94)
<i>t</i> BuCP	1573	1533 ^b	-0.52 (-1.11)	0.52 (0.93)
[(CF ₃) ₃ BCP] ⁻	1500	1468 ^b	-0.66 (-1.52)	0.41 (0.83)
<i>trans</i> -[Pt(PMe ₃) ₂ (Cl)(CP)]	1383	—	-0.85 (-1.20)	0.29 (0.71)
<i>trans</i> -[Pt(PMe ₃) ₂ (Cl)(CP)- Pt(PMe ₃) ₂]	1126	—	-1.00 (-1.31)	0.10 (0.54)
[(dppe) ₂ Ru(H)(CP)]	1270	1229 ^c	-0.76 (-1.31)	0.12 (0.54)

^a Reference 2. ^b Reference 27. ^c Reference 8.

is 1.566 Å long, equivalent to the other C≡P bond lengths, and that the C, Pt and Cl atoms lie on the same line. The frequency analysis retrieves a vibration at 1383 cm⁻¹ close to the HCP frequency.

Compound 7 in Figure 1 was synthesized⁷ from the unstable platinum complex 6 and was studied within this work. We were able to confirm the structural data established experimentally^{7a} that determined a bond length of 1.666(6) Å for the C≡P bond in comparison to the 1.657 Å calculated by us.

A ruthenium complex was also investigated, and structural information can be found in Figure 1. We obtained a C≡P bond distance of 1.582 Å which is slightly elongated relative to the experimental value⁸ found in literature of 1.573(2) Å. The vibrational frequency is in good agreement, being 1270 cm⁻¹ the calculated frequency and 1229 cm⁻¹ the experimental one.⁸ The complex here studied was modeled with methyl groups instead of the phenyl groups present in the synthesized compound.

All the results concerning frequencies and charges on the carbon and phosphorus atoms of the C≡P bond, obtained from the NPA and AIM analyses, are summarized in Table 1.

NBO analysis clearly confirms the existence of a triple bond between the C and P atoms for all the examined compounds (see below the discussion regarding compound 7). As an example, the σ -bond orbital obtained in the case of *t*BuCP is formed from hybrid orbitals on the C and P atoms: $\sigma(\text{CP}) = 0.81 (sp)_\text{C} + 0.59 (sp^{2.57})_\text{P}$, whereas the π -bond orbitals, $\pi(\text{CP}) = 0.74 (p)_\text{C} + 0.67 (p)_\text{P}$, are formed from pure p atomic orbitals. For the rest of the structures the C≡P bond description offered by NBO differs from the previous one in small variations of the polarization coefficients. We note that the polarization coefficients (0.81 for C and 0.59 for P) indicate that carbon, with the 65%, has the larger percentage of this NBO and gives the larger coefficient of 0.81. We note that in the case of the complex 7 the bonding description obtained by NBO is quite dependent on the basis sets quality. Indeed, some preliminary calculations performed by us at the B3LYP/6-31+G(d) level indicated that the C≡P bond (1.666 Å) was better described as a double bond. However, with the increase of the basis sets (B3LYP/6-311+G(2d,2p)) the NBO analysis character-

izes the bond between C and P atoms as a triple bond. The carbon atom is also bonded to the Pt(1) atom interacting with the Cl ligand. As a consequence, the bonding of C≡P with the Pt(2) atom (see Figure 1) can be described in terms of donor–acceptor interactions. NBO second-order perturbation analysis shows that the donation of the C≡P π electrons to the metal *d* orbitals is accompanied by π -backdonation from the metal *d* orbitals to the empty C≡P π^* orbital. Since the donation depopulates the π orbital of the ligand and the backdonation populates the ligand antibonding π^* , the C≡P bond of the ligand lengthens and its substituent bends away from the metal. Indeed, the C≡P bond is longer (1.657 Å) than in the rest of the examined compounds, and the P–C–Pt(2) bond angle is significantly distorted from linearity (143.3°).

The NPA Charge Analysis gives a -1 charge on CP⁻ concentrated on the C atom (-0.83 on C versus -0.17 on P). The C≡P bond is in all the other cases polarized as C^{δ-}–P^{δ+}. However, the negative charge existing on the C atom is always high, whereas the positive one on P atom significantly decreases when the ligand is coordinated to a metal center in stable complexes.

In Table 1 we have also included the atomic charges calculated within the AIM theory framework. The AIM theory provides a definition of atomic charges that is completely different from any other orbital-based population analysis. Atomic charges are obtained in this case by integration of the electron density within the atomic basins and adding the nuclear charges. Notably different values of the atomic charges were obtained with AIM, which predicts in all cases a larger charge separation. On the basis of the partition scheme used by AIM, we consider that AIM values are more reliable.

Table 2 summarizes the main information concerning C≡P bonds obtained by the topological analysis of the ELF function for all the studied species. In particular, we report the basin populations of the disynaptic V(C,P) and V(C,R) basins, which in terms of ELF analysis represent the CP bond and the second (and third in the case of compound 7) bond formed by that carbon atom, together with the corresponding variances, $\sigma^2(\tilde{N})$. We also report the monosynaptic V(P) basin populations, which represent the P lone pairs.

Figure 2 shows the ELF isosurfaces for CP⁻, HCP, CH₃CP, and *t*BuCP, whereas the rest of the structures are presented in Figure 3.

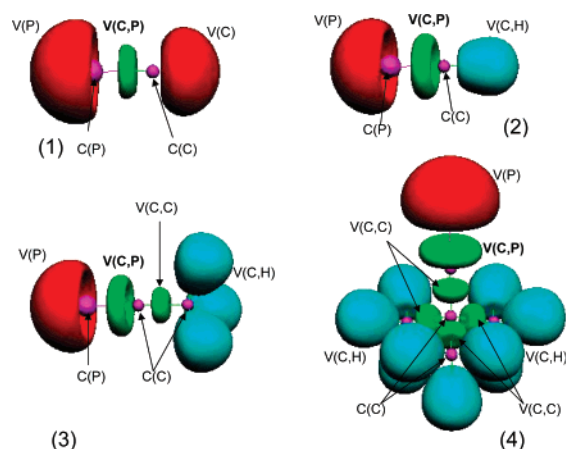
In the case of the two simplest species studied in this work, CP⁻ and HCP, the structures are characterized by the presence of a disynaptic valence basin, V(C,P), with an electron population of 2.91 and 4.07 e, respectively, together with monosynaptic V(P) basins with quite high populations (4.22 and 3.45 e, respectively). In both cases, we found strongly polarized disynaptic basins, as the atomic contribution coming from P atom is between 10 and 14% of the total population. Both valence basins are characterized by quite high variances, which indicate a great degree of electron delocalization. With the aim of comparison we have included the same data for CN⁻ and HCN as a footnote of Table 2.

Table 2. ELF Topological Properties: Electron Population of the V(C,P), V(C,R) and V(P) Valence Basins, Together with the Corresponding Variances, $\sigma^2(\bar{N})^a$

	V(C,P), $\sigma^2(\bar{N})$	V(C,R), $\sigma^2(\bar{N})$	V(P), $\sigma^2(\bar{N})$
CP [−]	2.91, 1.39	2.66, 0.9 ^b	4.22, 1.55
HCP	4.07, 1.57	2.31, 0.70 (R = H)	3.45, 1.35
CH ₃ CP	4.26, 2.70	2.15, 1.06 (R = C)	3.48, 1.35
tBuCP	4.19, 2.67	2.22, 1.10 (R = C)	3.53, 1.37
[(CF ₃) ₃ BCP] [−]	3.90, 2.66	2.37, 1.10 (R = B)	3.62, 1.40
<i>trans</i> -[Pt(PMe ₃) ₂ (Cl)(CP)]	3.73, 2.26	2.21, 1.28 (R = Pt)	3.89, 1.49
<i>trans</i> -[Pt(PMe ₃) ₂ (Cl)(CP)Pt(PMe ₃) ₂]	2.87, 1.47	1.94, 1.19 (R = Pt1) 1.50, 1.01 (R = Pt2)	4.68, 1.91
[(dppe) ₂ Ru(H)(CP)]	3.39, 1.55	2.50, 1.33 (R = Ru)	4.17, 1.57

^a All quantities are given in electrons. With the aim of comparison, the same data for CN[−] are as follows: V(C,N), $\sigma^2(\bar{N})$ = 3.39, 1.45; V(N), $\sigma^2(\bar{N})$ = 3.54, 1.27; V(C), $\sigma^2(\bar{N})$ = 2.86, 0.98; and for HCN: V(C,N), $\sigma^2(\bar{N})$ = 4.24, 1.54; V(N), $\sigma^2(\bar{N})$ = 3.28, 1.19; V(C,H), $\sigma^2(\bar{N})$ = 2.28, 0.67.

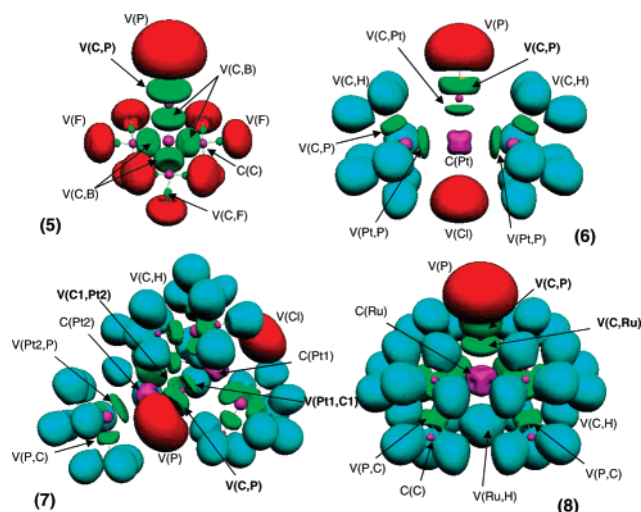
^b This value corresponds to the population and the variance of the monosynaptic V(C) basin.

**Figure 2.** ELF isosurfaces ($\eta(r)=0.8$) for the optimized structures of (1) CP[−]; (2) HCP; (3) CH₃CP; and (4) tBuCP. Core basins are represented in magenta, valence monosynaptic in red, protonated disynaptic in light blue; and valence disynaptic in green.

We have also reported the covariance matrix blocks, as obtained from TopMod package, in the Supporting Information.

Several studies present in bibliography have shown how the bond description obtained from ELF populations of multiple bonds involving atoms that contains lone pairs differs from our simplistic traditional pictures.^{28–30} Indeed, in the particular case of triple bonds, the bonding population is usually significantly lower than the formal value of six, at the expense of increased lone-pair population. The origin of the so-called lone-pair bond weakening effect (LPBWE) has been largely studied and has demonstrated its importance for all atoms.³¹ This subject has been analyzed in the context of Charge-Shift (CS) bonding and has been found that in ELF analysis it is manifested by a depleted basin population with a large variance and negative covariance. Based on Valence Bond Theory and ELF analysis calculations, it has been asserted that *triple bonding is invariably CS bonding*.³¹

The topological representation obtained from ELF analysis is usually interpreted in terms of superposition of mesomeric structures.^{28,29} In particular, a detailed description of the N₂ molecule²⁹ points out that the charge contributions of π orbitals to the V(N,N) bonding basin and V(N) lone pairs

**Figure 3.** ELF isosurfaces ($\eta(r)=0.75$) for the optimized structures of (5) [(CF₃)₃BCP][−]; (6) *trans*-[Pt(PMe₃)₂(Cl)(CP)]; (7) *trans*-[Pt(PMe₃)₂(Cl)(CP)Pt(PMe₃)₂]; and (8) [(dppe)₂Ru(H)(CP)] ($\eta=0.70$). Core basins are represented in magenta, valence monosynaptic in red, protonated disynaptic in light blue, and valence disynaptic in green.

are fairly equally shared. The results obtained here for CP[−] are in line with the previous study performed by Silvi and co-workers on the CN[−] and related series of compounds.³²

In the next three studied moieties, CH₃CP, tBuCP, and [(CF₃)₃BCP][−], we found disynaptic V(C,P) valence basins with decreasing electron populations of 4.26, 4.19, and 3.90 e, respectively. The contribution to the electron population coming from the P atom is in all cases around 10% of the total electron population. The lower electron population found in the case of [(CF₃)₃BCP][−] is caused by the fact that the carbon atom involved in the C≡P bond is also engaged in a C–B covalent bond. That bond is mainly formed from the contribution coming from the C atom, as indicated by the presence of a V(C,B) basin with a population of 2.37 e, to which the C atom contributes with 88% of the total population. In all the structures the monosynaptic V(P) basins show electron populations quite high, namely, around 3.50 e. The $\sigma^2(\bar{N})$ values are around 2.67 for V(C,P) basins and 1.37 in the case of V(P).

Table 3. AIM Topological Properties: Charge Density at the C–P Bond Critical Point, $\rho(\text{BCP})$, the Laplacian at the Same Point, $\nabla^2\rho(\text{BCP})$, the Ellipticity, ϵ , and the Delocalization Index, $\delta(\text{C,P})^a$

	$\rho(\text{BCP})^b$	$\nabla^2\rho(\text{BCP})^b$	ϵ	$\delta(\text{C,P})^c$
CP [−]	0.213	0.32	0.00	2.80
HCP	0.220	0.63	0.00	2.56
CH ₃ CP	0.214	0.63	2.9×10^{-6}	2.48
tBuCP	0.214	0.63	2.1×10^{-5}	2.46
[(CF ₃) ₃ BPC] [−]	0.220	0.59	9.9×10^{-5}	2.56
<i>trans</i> -[Pt(PMe ₃) ₂ (Cl)](CP)]	0.210	0.51	2.7×10^{-2}	2.42
<i>trans</i> -[Pt(PMe ₃) ₂ (Cl)](CP)-Pt(PMe ₃) ₂	0.190	0.16	0.09	1.76
[(dppe) ₂ Ru(H)](CP)	0.210	0.43	4.5×10^{-3}	2.44

^a With the aim of comparison the same data for CN[−] are as follows: $\rho(\text{BCP}) = 0.481$, $\nabla^2\rho(\text{BCP}) = -0.77$; $\epsilon = 0.00$, $\delta(\text{C,N}) = 2.40$ and for HCN: $\rho(\text{BCP}) = 0.453$, $\nabla^2\rho(\text{BCP}) = -0.51$, $\epsilon = 9.1 \times 10^{-8}$, $\delta(\text{C,N}) = 2.60$. ^b Electron density at the bond critical point and its Laplacian, are both in au. ^c The delocalization index, $\delta(\text{C,P})$, accounts for the electrons shared between the phosphorus and carbon atoms.

In the last three studied compounds, the C atom involved in the C≡P bond interacts also with a metal atom, as confirmed by the presence of a V(C,Ru) basin with a population of 2.50 e in [(dppe)₂Ru(H)](CP)] and a V(Pt,C) basin with 2.21 e in *trans*-[Pt(PMe₃)₂(Cl)](CP)]. In both cases the main contribution to that populations comes from the C atom (around 85%). In [(dppe)₂Ru(H)](CP)] and *trans*-[Pt(PMe₃)₂(Cl)](CP)] we found disynaptic V(C,P) basins, with total electron populations of 3.39 and 3.73 e, respectively. As in the previous cases the variances of these basins are quite high (see Table 2).

Finally, in compound 7, we found a V(C,P) valence basin with an electron population of 2.87 e. The electron population of the V(C,P) is quite depleted with respect to the previously described structures. This is due to the fact that according to ELF analysis the C atom interacts with both Pt atoms, as demonstrated by the presence of the V(Pt1,C1) and V(Pt2,-C1) valence basins with electron populations of 1.94 and 1.50 e (see Figure 3 and Figure S1 in the Supporting Information), respectively. In both cases, the electron population is mainly brought by the C atom (around 80%). We have, therefore, some contrasting bond descriptions of compound 7. ELF analysis indicates that the central carbon atom is tricoordinated and that the CP bond can be described as a double bond, whereas NBO analysis performed at the B3LYP/6-311+G(2d,2p) level of theory shows that the C atom forms a covalent bond only with the closest Pt atom (the Pt1C bond length is 1.974 Å, whereas the Pt2C distance is 2.092 Å). As shown below, based on the CP bond ellipticity, we conclude that AIM analysis supports the bonding description obtained by ELF calculations.

The properties of the (3, −1) bond critical points are reported in Table 3. In particular, we present the electron density, $\rho(\text{BCP})$, the Laplacian, $\nabla^2\rho(\text{BCP})$, the ellipticity, ϵ , and the delocalization index, $\delta(\text{C,P})$.

All C≡P BCPs display a significant concentration of electrons, with $\rho(\text{BCP})$ values ranging from 0.190 to 0.220 au. The BCP properties show that the nature of C≡P interactions is similar in all the studied structures. Significant values of $\rho(\text{BCP})$ along with values of $\nabla^2\rho(\text{BCP}) > 0$ and

$|\lambda_1/\lambda_3| < 1$ point to an interaction intermediate to closed-shell and shared nature. This description of the CP bond agrees with the atomic contributions to the V(C,P) basins obtained by ELF analysis, which shows a highly polarized bond. For the smaller structures, compounds 1–5, the ellipticity of the C≡P bond is zero or very close to zero (Table 3), whereas in the metal-containing complexes, that values slightly increase with the greatest value found in the case of complex 7, for which that value rises to 0.09.

4. Conclusions

In this paper, we have performed a comparative analysis of the bonding description obtained using different methodologies (ELF, AIM, NBO) of a series of compounds containing a terminal cyaphide bond.

The main conclusions drawn from this study can be summarized as follows:

1. The ELF V(C,P) basin populations obtained for all the studied species are characteristics of multiple bonds in which lone pairs are also involved. Moreover, in all the studied compounds, with the only exception of complex 7, the bonding basins have the axial symmetry characteristic of the triple bonds that yields a unique disynaptic basin which attractor is degenerated in a circle perpendicular to the C_∞ axis. In the case of compound 7 the V(C,P) bonding population is comparable to that obtained for CP[−]; however, the shape of the bonding basin resembles more the prolate spheroid basins characteristic of double bonds. Moreover, according to ELF analysis the C atom involved in the compound 7 CP bond interacts with both Pt atoms through the formation of polarized covalent bonds. ELF analysis shows C≡P bonds that are highly polarized in nature.

2. AIM analysis indicates that in all the studied compounds the $\rho(\text{BCP})$ at the C≡P BCP is around 0.2 au. A slightly lower value was found in the case of complex 7. Those values are almost half of the corresponding values in CN[−] and HCN, at the same level of theory. All the studied C≡P BCPs are characterized by small positive values of $\nabla^2\rho(\text{BCP})$, in contrast to CN[−] and HCN which values are small and negative. For all the studied systems, the CP bond ellipticities are zero or very close to zero, with the only exception of compound 7, for which that value rises to 0.09.

3. NBO analysis generally supports the description obtained by ELF indicating the presence of a C≡P triple bond in all the studied species. In all cases, the polarity of the C≡P bond, as evaluated from the NBO polarization coefficients, is generally less marked than that obtained from ELF analysis considering the different atomic contributions to the disynaptic V(C,P) basins.

4. The used level of theory has generally well reproduced the experimental, geometrical, and spectroscopic properties as well as previous theoretical results.

Financial support from the Università degli studi della Calabria is gratefully acknowledged. N.R. thanks the HPC-Europe for the grant IDRIS-62007.

Supporting Information Available: Cartesian coordinates of fully optimized compounds 1–8, covariance matrix blocks of ELF analysis, and an additional image of

the ELF basins of compound 7 (Figure S1). This material is available free of charge via the Internet at <http://pubs.acs.org>.

References

- (1) Jutzi, P. *Angew. Chem.* **1975**, 87, 269–283. Jutzi, P. *Angew. Chem., Int. Ed.* **1975**, 14, 232–245.
- (2) Gier, T. E. *J. Am. Chem. Soc.* **1961**, 83, 1769–1770.
- (3) Becker, G.; Gresser, G.; Uhl, W. Z. *Naturforsch., B: Chem. Sci.* **1981**, 36B, 16–19.
- (4) Regitz, M. *Chem. Rev.* **1990**, 90, 191–213.
- (5) (a) Nixon, J. F. *Chem. Rev.* **1988**, 88, 1327–1362. (b) Ehlers, A.; Cordaro, J. G.; Stein, D.; Grützmacher, H. *Angew. Chem., Int. Ed.* **2007**, 46, 7878–7881. (c) Angelici, R. J. *Angew. Chem., Int. Ed.* **2007**, 46, 330–332.
- (6) Weber, L. *Eur. J. Inorg. Chem.* **2003**, 1843–1856.
- (7) (a) Jun, H.; Angelici, R. J. *Organometallics* **1994**, 13, 2454–2460. (b) Jun, H.; Young, V. G., Jr.; Angelici, R. J. *J. Am. Chem. Soc.* **1992**, 114, 10064–10065.
- (8) Cordaro, J. G.; Stein, D.; Ruegger, H.; Grützmacher, H. *Angew. Chem., Int. Ed.* **2006**, 45, 6159–6162.
- (9) (a) Nguyen, M. T.; Ha, T.-K.; *J. Mol. Struct. (THEOCHEM)* **1986**, 139, 145–152. (b) Pykkö, P.; Zhao, Y. *Mol. Phys.* **1990**, 70, 701–714.
- (10) (a) Hübler, K.; Schwerdtfeger, P. *Inorg. Chem.* **1999**, 38, 157–164. (b) Kurita, E.; Tomonaga, Y.; Matsumoto, S.; Ohno, K.; Matsuura, H. *J. Mol. Struct. (THEOCHEM)* **2003**, 639, 53–67. (c) Pascoli, G.; Lavendy, H. *J. Phys. Chem. A* **1999**, 103, 3518–3524. (d) Mó, O.; Yanez, M.; Guillemin, J.-C.; Riague, E. H.; Gal, J.-F.; Maria, P.-C.; Poliart, C. D. *Chem. Eur. J.* **2002**, 8, 4919–4924.
- (11) Frisch, M. J.; Trucks, G. W.; Schlegel, H. B.; Scuseria, G. E.; Robb, M. A.; Cheeseman, J. R.; Montgomery, J. A., Jr.; Vreven, T.; Kudin, K. N.; Burant, J. C.; Millam, J. M.; Iyengar, S. S.; Tomasi, J.; Barone, V.; Mennucci, B.; Cossi, M.; Scalmani, G.; Rega, N.; Petersson, G. A.; Nakatsuji, H.; Hada, M.; Ehara, M.; Toyota, K.; Fukuda, R.; Hasegawa, J.; Ishida, M.; Nakajima, T.; Honda, Y.; Kitao, O.; Nakai, H.; Klene, M.; Li, X.; Knox, J. E.; Hratchian, H. P.; Cross, J. B.; Bakken, V.; Adamo, C.; Jaramillo, J.; Gomperts, R.; Stratmann, R. E.; Yazyev, O.; Austin, A. J.; Cammi, R.; Pomelli, J. MoC.; Ochterski, J. W.; Ayala, P. Y.; Morokuma, K.; Voth, G. A.; Salvador, P.; Dannenberg, J. J.; Zakrzewski, V. G.; Dapprich, S.; Daniels, A. D.; Strain, M. C.; Farkas, O.; Malick, D. K.; Rabuck, A. D.; Raghavachari, K.; Foresman, J. B.; Ortiz, J. V.; Cui, Q.; Baboul, A. G.; Clifford, S.; Cioslowski, J.; Stefanov, B. B.; Liu, G.; Liashenko, A.; Piskorz, P.; Komaromi, I.; Martin, R. L.; Fox, D. J.; Keith, T.; Al-Laham, M. A.; Peng, C. Y.; Nanayakkara, A.; Challacombe, M.; Gill, P. M. W.; Johnson, B.; Chen, W.; Wong, M. W.; Gonzalez, C.; Pople, J. A. *Gaussian 03, Revision C.02*; Gaussian, Inc.: Wallingford, CT, 2004.
- (12) Becke, A. D. *J. Chem. Phys.* **1993**, 98, 5648–5652.
- (13) Stephens, P. J.; Devlin, F. J.; Chabalowski, C. F.; Frisch, M. J. *J. Phys. Chem.* **1994**, 98, 11623–11627.
- (14) Wadt, W. R.; Hay, P. J. *J. Chem. Phys.* **1985**, 82, 284–298.
- (15) (a) Krishnan, R.; Binkley, J. S.; Seeger, R.; Pople, J. A. *J. Chem. Phys.* **1980**, 72, 650–654. (b) Blaudeau, J.-P.; McGrath, M. P.; Curtiss, L. A.; Radom, L. *J. Chem. Phys.* **1997**, 107, 5016–5021.
- (16) (a) Reed, A. E.; Weinhold, F. *J. Chem. Phys.* **1985**, 83, 1736–1740. (b) Reed, A. E.; Curtiss, L. A.; Weinhold, F. *Chem. Rev.* **1988**, 88, 899–926.
- (17) Becke, A. D.; Edgecombe, K. E. *J. Chem. Phys.* **1990**, 92, 5397–5403.
- (18) Silvi, B.; Savin, A. *Nature* **1994**, 371, 683–686.
- (19) (a) Noury, S.; Krokidis, X.; Fuster, B. Silvi, B. *TopMod Package*; Paris, 1997. (b) Noury, S.; Krokidis, X.; Fuster, F.; Silvi, B. *Comput. Chem.* **1999**, 23, 597–604.
- (20) Bader, R. F. *Atoms in molecules. A quantum theory*; Clarendon: Oxford, 1990.
- (21) (a) Cremer, D.; Kraka, E.; Slee, T. S.; Bader, R. F. W.; Lau, C. D. H.; Nguyen-Dang, T. T.; McDougall, P. J. *J. Am. Chem. Soc.* **1983**, 105, 5069–5075. (b) Bader, R. F. W.; Slee, T. S.; Cremer, D.; Kraka, E. *J. Am. Chem. Soc.* **1983**, 105, 5061–5068. (c) Scherer, W.; Sirsch, P.; Shorokhov, D. M. Tafipolsky, M.; McGrady, G. S.; Gullo, E. *Chem. Eur. J.* **2003**, 9, 6057–6070.
- (22) (a) Fradera, X.; Austen, M. A.; Bader, R. F. W. *J. Phys. Chem. A* **1999**, 103, 304–314. (b) Fradera, X.; Poater, J.; Simon, S.; Duran, M.; Solà, M. *Theor. Chem. Acc.* **2002**, 108, 214–224.
- (23) Ágáyán, J. G.; Loos, M.; Mayer, I. *J. Phys. Chem.* **1994**, 98, 5244–5248.
- (24) Poater, J.; Duran, M.; Solà, M.; Silvi, B. *Chem. Rev.* **2005**, 105, 3911–3947, and references therein.
- (25) (a) Lavigne, J.; Pepin, C.; Cabana, A. *J. Mol. Spectrosc.* **1984**, 104, 49–58. (b) Kroto, H. W.; Nixon, J. F.; Simmons, N. P. *C. J. Mol. Spectrosc.* **1979**, 77, 270–285.
- (26) Antipin, M. Y.; Chernega, A. N.; Lysenko, K. A.; Struchkov, Y. T.; Nixon, J. F. *J. Chem. Soc., Chem. Commun.* **1995**, 505–506.
- (27) Finze, M.; Bernhardt, E.; Willner, H.; Lehmann, C. W. *Angew. Chem., Int. Ed.* **2004**, 43, 4160–4163.
- (28) (a) Silvi, B. *Phys. Chem. Chem. Phys.* **2004**, 6, 256–260. (b) Lepetit, C.; Silvi, B.; Chauvin, R. *J. Phys. Chem. A* **2003**, 107, 464–473.
- (29) Pilme, J.; Silvi, B.; Alikhani, M. E. *J. Phys. Chem. A* **2005**, 109, 10028–10037.
- (30) (a) Silvi, B.; Fourré, I.; Alikhani, M. E. *Monatsh. Chem.* **2005**, 136, 855–879. (b) Chesnut, D. B. *Heteroat. Chem.* **2000**, 11, 341–352.
- (31) Shaik, S.; Danovich, D.; Silvi, B.; Lauvergnat, D. L.; Hiberty, P. C. *Chem. Eur. J.* **2005**, 11, 6358–6371, and references therein.
- (32) Matito, E.; Silvi, B.; Duran, M.; Solà, M. *J. Chem. Phys.* **2006**, 125, 024301-9.

CT700277W